

Mapping Single-Molecule Protein Complexes in 3D with DNA Nanoswitch Calipers

Prakash Shrestha, Darren Yang, Andrew Ward, William M. Shih, and Wesley P. Wong*

 Cite This: *J. Am. Chem. Soc.* 2023, 145, 27916–27921

 Read Online

ACCESS |

 Metrics & More

 Article Recommendations

 Supporting Information

ABSTRACT: The ability to accurately map the 3D geometry of single-molecule complexes in trace samples is a challenging goal that would lead to new insights into molecular mechanics and provide an approach for single-molecule structural proteomics. To enable this, we have developed a high-resolution force spectroscopy method capable of measuring multiple distances between labeled sites in natively folded protein complexes. Our approach combines reconfigurable nanoscale devices, we call DNA nanoswitch calipers, with a force-based barcoding system to distinguish each measurement location. We demonstrate our approach by reconstructing the tetrahedral geometry of biotin-binding sites in natively folded streptavidin, with 1.5–2.5 Å agreement with previously reported structures.

The ability to determine the spatial organization of biomacromolecular complexes has led to new insights into biological mechanism and therapeutic development.^{1,2} Despite advances in computational tools for predicting protein structure,^{3–5} challenges remain in the prediction of multi-protein complex assembly, mechanical properties, and conformational transitions. Technologies such as super-resolution microscopy^{6–9} and structural biology methods such as cryoEM^{10–12} have opened new avenues for measurement, yet applications to fields such as proteomics have been constrained due to limitations in resolution, accuracy, and throughput on one hand, and the challenge of working with trace, heterogeneous samples on the other. Emerging single-molecule approaches show promise, as single-molecule fluorescence resonance energy transfer (smFRET),^{13–16} force spectroscopy,^{17–20} and nanopore²¹ methods have been used to study biomolecular geometry and dynamics. AFM studies have demonstrated reconstruction of folded protein geometry,^{22,23} although measurements were largely limited to a single pairwise distance per molecule. Resolving the challenge of making multiple atomically precise distance measurements within natively folded single-biomolecular complexes could enable applications in single-molecule proteomics, including three-dimensional geometry determination from trace samples and studies of molecular interactions, heterogeneity, and structure–function relationships.

To enable this, we developed an approach that combines reconfigurable nanodevices with single-molecule force spectroscopy. We previously introduced DNA nanoswitch calipers (DNC) and demonstrated applications to protein–sequence fingerprinting by measuring the distances between specific residues within denatured peptides, chemically labeled with DNA handles.²⁴ Each DNC consists of a DNA tether containing a pair of grabber sequences complementary to the DNA handles on an analyte of interest; when these grabbers engage two handles on an analyte, a section of DNA loops out (Figure 1). When sufficient force is applied to the DNC tether

at its two ends, one grabber is released, and the change-in-distance between the two ends reports the distance between handles. Here, by combining DNC with force-based barcodes to augment our ability to disambiguate labeled sites, we measure the distances between multiple coordinates on the surface of an intact, natively folded protein complex and reconstruct the three-dimensional geometry of these coordinates (Figure 1). As a demonstration, we reconstruct the geometry of biotin-binding sites in streptavidin by measuring pairwise distances between binding sites, using symmetry to calculate their relative positions in 3D space. Streptavidin is a tetramer consisting of four identical, noncovalently attached units,²⁵ in which biotin-binding sites form an irregular tetrahedron with opposite sides of equal length^{26,27} (Figure 2A).

As a first step in validating our approach, we used DNC to measure a single distance between pairs of biotin-binding sites for each single-molecule complex (Figure 2). We first loaded one long biotinylated ssDNA strong handle and one short biotinylated ssDNA weak handle on each caliper and then added tetrameric streptavidin for bivalent capture (Figures 2 and S1). The shearing force of the weak handle in our experiments (~26 pN) was significantly lower than the biotin–streptavidin unbinding force,^{28–31} so the biotin oligonucleotide generally remained attached to the streptavidin complex. Within each measurement cycle, force was applied to each DNC using optical tweezers and varied between a low force and a high force; at the high force of ~26 pN, a sudden change in extension (ΔL) results from shearing of the weak handle,

Received: September 19, 2023

Revised: December 11, 2023

Accepted: December 12, 2023

Published: December 14, 2023



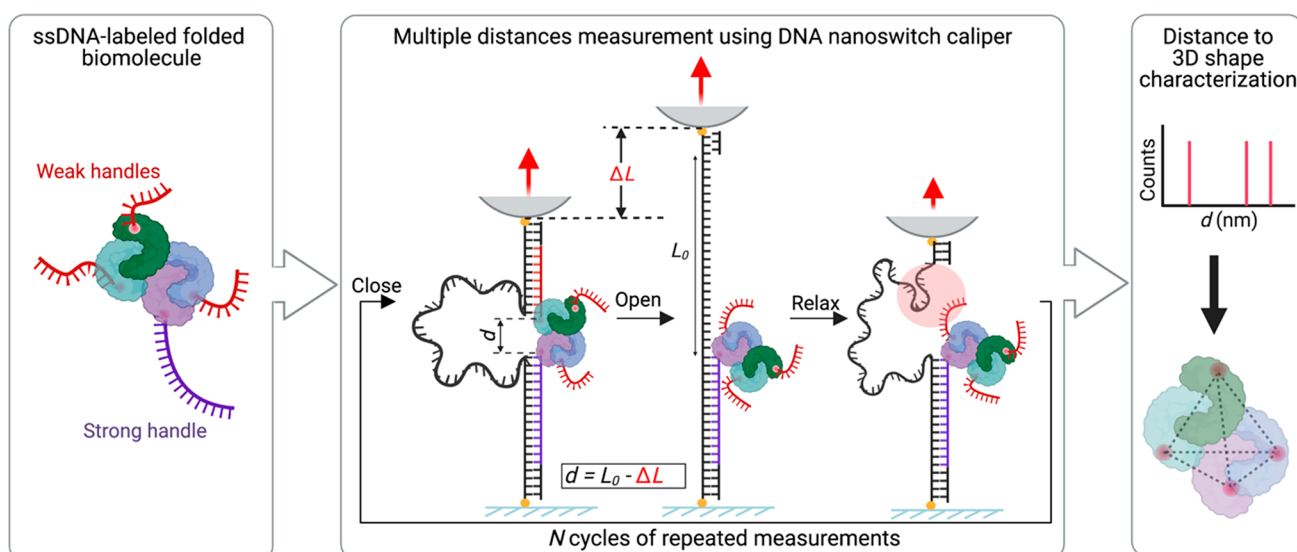


Figure 1. Overview of single-molecule 3D mapping with DNA nanoswitch calipers (DNC). (Left) Natively folded biomolecular complex labeled with ssDNA handles: a strong handle (purple) that serves as an anchoring site for DNC and shorter weak handles (red). (Middle) Multiple distances are measured between red and purple handles using a DNC actuated by mechanical force. Each DNC has one “grabber” complementary to the weak handles and one complementary to the strong handle. As force is cycled between low and high forces, the caliper alternates between looped and linear states, due to engagement then release of the weak handle. (Top right) Distribution of measured distances d calculated by subtracting the change in length ΔL from the effective loop length L_0 , which serves as a reference to convert changes in length to absolute distance. (Bottom right) Reconstructed geometry for positions of DNA-labeled sites in the folded biomolecular complex.

and at the low force of ~ 0 pN, rebinding of the weak handle occurs, relooping the DNC tether (Figure 2C–E). The effective loop length (L_0) was determined by performing calibration measurements of the DNC constructs at the distance-measuring force;²⁴ the distance d was then calculated as $d = L_0 - \Delta L$ (see Methods and Figure 2C). Analyzing the distance distribution of each molecule (e.g., Figure 2F) yields a single distance for each, which when aggregated over multiple molecules shows three distances as expected (Figures 2G and S2). Assuming an irregular tetrahedron with D2 dihedral symmetry, as indicated from X-ray crystallography,³² we used these distances to reconstruct the three-dimensional geometry of the biotin-binding sites of streptavidin (Supplementary Note 1), closely matching the previously established structure (RMSD = 1.54 Å) (Figures 2H and S3).

While systems such as biotin–streptavidin are relatively robust and able to withstand the ~ 26 pN forces exerted during measurement, lower forces may be needed to study more labile molecular complexes. To demonstrate the ability of DNC to study less mechanically stable structures, we performed distance measurements on the folded DNA G-quadruplex structure, which has been shown to denature at ~ 20 pN,¹⁸ using shorter ssDNA weak handles to reduce the force applied. By tuning the length of the weak handles to 9 bases, which can be sheared at ~ 10 pN during DNC measurements, we measured the 5′–3′ distance in the folded structure in the presence of potassium ions and obtained results that agreed with the expected G-quadruplex structure³³ (PDB 2HY9) (Figure S4).

Next, to enable the measurement of multiple distances per single-molecule complex, we developed a barcoding system that enabled each binding site to be identified based on force–extension behavior. This increases the resolution of DNC measurements by enabling handles that are closer than the resolution of a single distance measurement to be distinguished, with increased localization precision obtained by

averaging repeated distance measurements, in the spirit of super-resolution approaches such as PALM,⁹ FPALM,³⁴ and STORM.³⁵ Here, we used hairpin barcodes in the weak handles to help resolve all distances between biotin-binding sites in a single-streptavidin molecule. We incorporated long, short, and “no hairpin” structures in the weak handles, with hairpin-unfolding length serving as a barcode (Figure 3A,B). Constructs were assembled in a similar manner to that before but with subsequent incubation with barcoded biotinylated weak handles so that biotin-binding sites were fully occupied (see Methods and Figure S5). This yielded a distribution of molecules with either unique or degenerate barcodes, leading to some variation in the total number of unique distances and barcodes we could measure on each molecule. We slowly ramped the force up to ~ 15 pN to probe hairpin unfolding, jumped to moderate force (~ 20 pN) to measure the distance between biotin-binding sites, jumped to high force (~ 30 pN) to shear open the DNC loop, and then jumped back to moderate force to determine the change in length (~ 20 pN) (Figure 3C–E). The effective loop length (L_0) of the DNC at the moderate distance measuring force was determined as previously described²⁴ and used to calculate the absolute distance d (Figure S6). Repetitive cycles of force application in each streptavidin–biotin complex enabled us to observe the stochastic binding of all weak handles (Figure 3E,F and Figures S7 and S8) and determine their distances from the strong handle.

Aggregating all of the distances measured over different molecules, which were bound with different numbers of DNA handles, yields a distance distribution that shows three primary peaks at the expected distances (Figure 3G). As in our previous example, by analyzing these three distances in light of the expected irregular tetrahedral symmetry, we can reconstruct the three-dimensional geometry of the biotin-binding sites in streptavidin. As before, the geometry of the binding sites

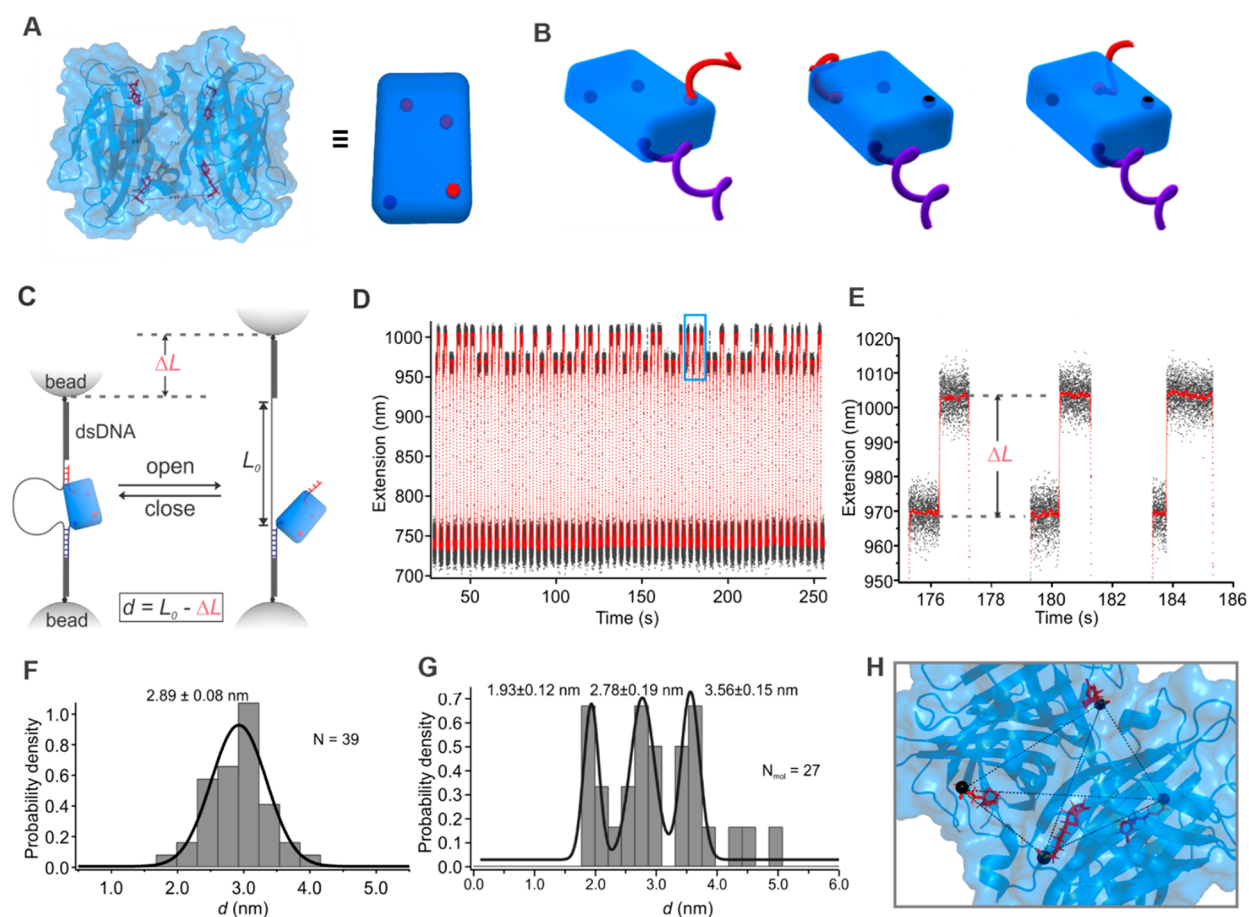


Figure 2. Single-molecule distance measurements of streptavidin–biotin complexes with only two biotin sites occupied. (A) Structure of streptavidin–biotin complex (PDB entry 6M9B) (left) with a schematic representation (right) where spheres indicate biotins bound to streptavidin. (B) Schematic of streptavidin bound to two biotinylated ssDNA handles illustrating three distinct configurations. The longer (purple) strong handle provides strong attachment to the DNC, while the shorter (red) weak handle shears off at lower force. Biotinylated handles are hybridized to the DNC construct prior to the introduction of streptavidin to yield one pair of handles per molecule (Figure S1). (C) DNC tethered between two optically trapped microbeads and actuated by force to measure distances between biotin-binding sites in streptavidin. DNC looping occurs when both handles are engaged; unlooping occurs when the weak handle shears off at high force; relooping occurs with weak handle rebinding at low force. (D) Data showing DNC extension over cycles of low and high force (raw data in black, 200-point sliding window average in red). (E) Zoom-in of blue rectangle in D, showing change in extension due to DNC unlooping. (F) Distance histogram calculated by subtracting ΔL from effective loop length (L_0). (G) Histogram of per-molecule average distances for 27 molecular complexes. Plus–minus values indicate sigma fitting parameters from the multipeak Gaussian fit. (H) DNC determined positions of carbon in the carboxylic group of each biotin (black spheres) superimposed on the crystal structure (PDB 6M9B).

determined using DNC agrees closely with measurements from X-ray crystallography (RMSD 2.34 Å) (Figures 3H and S9).

While we used symmetry here to aid in geometric reconstruction, using computational analysis, we also explored whether reconstruction could be accomplished without this prior knowledge. We simulated DNC measurements, using the known crystal structure as the ground truth, to determine how well the expected 3D geometry of the biotin–streptavidin complex could be recovered from a set of all pairwise distance measurements, where full incorporation of barcodes enables all handles to be uniquely identified. As described in Figure S10 and Supplementary Note 2, we find that reconstruction from the assigned Euclidean distance matrix (EDM)³⁶ does a reasonably good job of recovering the ground truth provided the measurement resolution is sufficient.

Interestingly, we found in our experiments that when a single streptavidin complex was fully occupied by biotinylated DNA handles, the apparent distance between the two closest biotin-binding sites was shorter than expected (Figure 3F). To

further investigate, we performed additional experiments in which only one distance per complex was measured through attached DNA–biotin handles, while the remaining two biotin-binding sites were putatively occupied by biotin (Figure S11). We again found a population exhibiting shorter than expected distances (Figures S12 and S13), confirming our observation that when the streptavidin complex has all sites occupied, it can exhibit subtly different physical properties than when only two sites are occupied. As described in Supplementary Note 3 and Figure S14, differences in the structural properties of free vs biotin-bound streptavidin^{27,37} could contribute to a shorter apparent length between the two closest biotin-binding sites.

In summary, we have developed a technique to measure multiple distances on natively folded single-molecule complexes using barcodes to enhance the spatial resolution of DNC on a per-molecule basis and help facilitate 3D reconstruction. We measured the distances between biotin-binding sites in a streptavidin molecule using three hairpin barcodes as a proof-of-concept example. We successfully

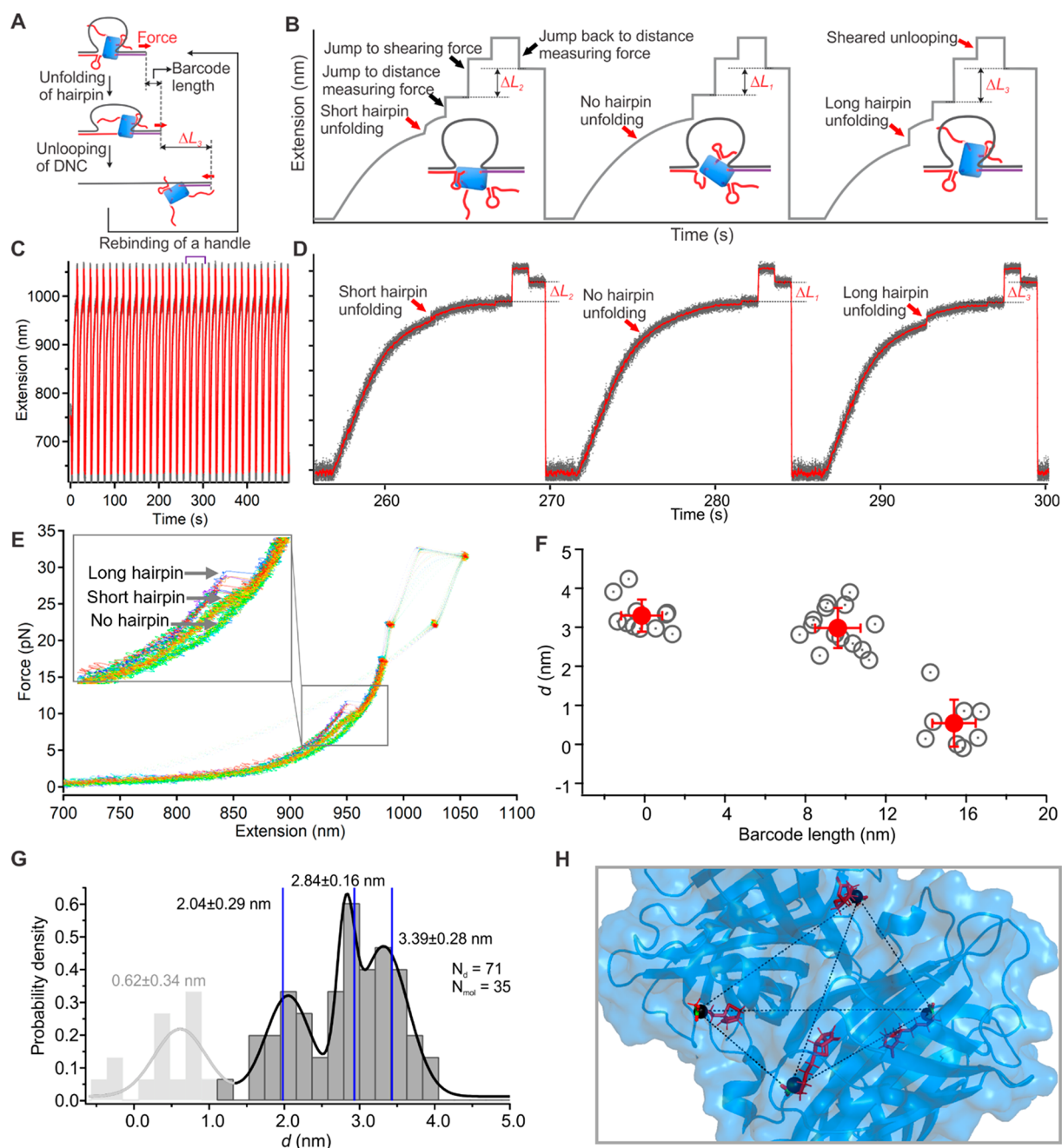


Figure 3. 3D mapping of streptavidin–biotin complex with force-based barcodes to resolve multiple distance measurements per molecule. (A) Schematic showing incorporation and readout of hairpin barcodes incorporated into weak handles (red). First, hairpin opening enables handle identification from the change in length, and then loop opening at a higher force enables the distance between handles to be measured as before. Dropping the force enables rebinding to another handle. (B) Outline of distance measurement strategy consisting of a force ramp for hairpin readout, followed by jumps in force to ~ 20 pN to measure the distance, ~ 30 pN to shear the weak handle, ~ 20 pN to measure the change in length, and then ~ 0 pN to enable rebinding. Three cycles are shown, illustrating unfolding signatures of the three barcodes. (C) Extension vs time data for a DNC over multiple force cycles (raw data in gray, smoothed in red). (D) Zoom-in of a section (indicated by purple arrows) from C depicting the sequential readout of all three barcodes. (E) Force vs extension curves of repeated cycles depicting the measurement of all three barcode lengths in one streptavidin molecule. (F) Scatter plot of measured barcode lengths vs handle distances in a single molecule. For each cluster, red circles indicate mean, and error bars indicate standard deviation. (G) Histogram of per-molecule distances aggregated over multiple molecules. Plus–minus values indicate sigma fitting parameters from the multipeak Gaussian fit. Blue vertical lines indicate expected distances between biotin-binding sites based on the crystal structure (PDB 6M9B). (H) Superposition of the DNC determined the position of the carbon in the carboxylic group of each biotin (black spheres) on the crystal structure.

reconstructed the three-dimensional tetrahedron geometry of biotin-binding sites in the streptavidin molecule, which agrees closely (RMSD 2.34 Å) with that determined from X-ray crystallography. DNC is a powerful and accessible technique to

study the three-dimensional positions of residues in single biomolecules or biomolecular complexes that should lead to new applications in single-molecule proteomics, including the determination of three-dimensional molecular conformations

from trace biological samples and the discovery of new biomarkers for diagnostics and allosteric modulators for therapeutics.

■ ASSOCIATED CONTENT

SI Supporting Information

The Supporting Information is available free of charge at <https://pubs.acs.org/doi/10.1021/jacs.3c10262>.

Methods, Supplementary Table 1, Supplementary Figures S1–S14, and Supplementary Notes 1–3 (PDF)

■ AUTHOR INFORMATION

Corresponding Author

Wesley P. Wong – Program in Cellular and Molecular Medicine, Boston Children's Hospital, Boston, Massachusetts 02115, United States; Wyss Institute for Biologically Inspired Engineering, Harvard University, Boston, Massachusetts 02215, United States; Department of Biological Chemistry and Molecular Pharmacology, Blavatnik Institute, Harvard Medical School, Boston, Massachusetts 02115, United States; orcid.org/0000-0001-7398-546X; Email: Wesley.Wong@childrens.harvard.edu

Authors

Prakash Shrestha – Program in Cellular and Molecular Medicine, Boston Children's Hospital, Boston, Massachusetts 02115, United States; Wyss Institute for Biologically Inspired Engineering, Harvard University, Boston, Massachusetts 02215, United States; Department of Biological Chemistry and Molecular Pharmacology, Blavatnik Institute, Harvard Medical School, Boston, Massachusetts 02115, United States; orcid.org/0000-0002-7914-7122

Darren Yang – Program in Cellular and Molecular Medicine, Boston Children's Hospital, Boston, Massachusetts 02115, United States; Wyss Institute for Biologically Inspired Engineering, Harvard University, Boston, Massachusetts 02215, United States; Department of Biological Chemistry and Molecular Pharmacology, Blavatnik Institute, Harvard Medical School, Boston, Massachusetts 02115, United States

Andrew Ward – Program in Cellular and Molecular Medicine, Boston Children's Hospital, Boston, Massachusetts 02115, United States; Wyss Institute for Biologically Inspired Engineering, Harvard University, Boston, Massachusetts 02215, United States

William M. Shih – Wyss Institute for Biologically Inspired Engineering, Harvard University, Boston, Massachusetts 02215, United States; Department of Cancer Biology, Dana-Farber Cancer Institute, Boston, Massachusetts 02215, United States; Department of Biological Chemistry and Molecular Pharmacology, Blavatnik Institute, Harvard Medical School, Boston, Massachusetts 02115, United States; orcid.org/0000-0002-1395-9267

Complete contact information is available at:

<https://pubs.acs.org/doi/10.1021/jacs.3c10262>

Notes

The authors declare the following competing financial interest(s): W.M.S. and W.P.W. have filed patent applications for various aspects of this work.

■ ACKNOWLEDGMENTS

This work was funded by support from ONR Award N000141510073, NIH NIGMS R35 GM119537 (W.P.W.), Alfred P. Sloan Foundation Award G-2021-169145, and the Wyss Institute at Harvard. The authors acknowledge that some figures were prepared using BioRender.

■ REFERENCES

- (1) Thomas, S. E.; Mendes, V.; Kim, S. Y.; Malhotra, S.; Ochoa-Montaño, B.; Blaszczyk, M.; Blundell, T. L. Structural Biology and the Design of New Therapeutics: From HIV and Cancer to Mycobacterial Infections: A Paper Dedicated to John Kendrew. *J. Mol. Biol.* **2017**, *429* (17), 2677–2693.
- (2) Engelman, A.; Cherepanov, P. The Structural Biology of HIV-1: Mechanistic and Therapeutic Insights. *Nat. Rev. Microbiol.* **2012**, *10* (4), 279–290.
- (3) Jumper, J.; Evans, R.; Pritzel, A.; Green, T.; Figurnov, M.; Ronneberger, O.; Tunyasuvunakool, K.; Bates, R.; Židek, A.; Potapenko, A.; Bridgland, A.; Meyer, C.; Kohli, S. A. A.; Ballard, A. J.; Cowie, A.; Romera-Paredes, B.; Nikolov, S.; Jain, R.; Adler, J.; Back, T.; Petersen, S.; Reiman, D.; Clancy, E.; Zielinski, M.; Steinegger, M.; Pacholska, M.; Berghammer, T.; Bodenstein, S.; Silver, D.; Vinyals, O.; Senior, A. W.; Kavukcuoglu, K.; Kohli, P.; Hassabis, D. Highly Accurate Protein Structure Prediction with AlphaFold. *Nature* **2021**, *596* (7873), 583–589.
- (4) Tunyasuvunakool, K.; Adler, J.; Wu, Z.; Green, T.; Zielinski, M.; Židek, A.; Bridgland, A.; Cowie, A.; Meyer, C.; Laydon, A.; Velankar, S.; Kleywegt, G. J.; Bateman, A.; Evans, R.; Pritzel, A.; Figurnov, M.; Ronneberger, O.; Bates, R.; Kohli, S. A. A.; Potapenko, A.; Ballard, A. J.; Romera-Paredes, B.; Nikolov, S.; Jain, R.; Clancy, E.; Reiman, D.; Petersen, S.; Senior, A. W.; Kavukcuoglu, K.; Birney, E.; Kohli, P.; Jumper, J.; Hassabis, D. Highly Accurate Protein Structure Prediction for the Human Proteome. *Nature* **2021**, *596* (7873), 590–596.
- (5) Bradley, P.; Misura, K. M. S.; Baker, D. Toward High-Resolution de Novo Structure Prediction for Small Proteins. *Science* **2005**, *309* (5742), 1868–1871.
- (6) Sigal, Y. M.; Zhou, R.; Zhuang, X. Visualizing and Discovering Cellular Structures with Super-Resolution Microscopy. *Science* **2018**, *361* (6405), 880–887.
- (7) Sahl, S. J.; Hell, S. W.; Jakobs, S. Fluorescence Nanoscopy in Cell Biology. *Nat. Rev. Mol. Cell Biol.* **2017**, *18* (11), 685–701.
- (8) Jungmann, R.; Steinhauer, C.; Scheible, M.; Kuzyk, A.; Tinnefeld, P.; Simmel, F. C. Single-Molecule Kinetics and Super-Resolution Microscopy by Fluorescence Imaging of Transient Binding on DNA Origami. *Nano Lett.* **2010**, *10* (11), 4756–4761.
- (9) Betzig, E.; Patterson, G. H.; Sougrat, R.; Lindwasser, O. W.; Olenych, S.; Bonifacino, J. S.; Davidson, M. W.; Lippincott-Schwartz, J.; Hess, H. F. Imaging Intracellular Fluorescent Proteins at Nanometer Resolution. *Science* **2006**, *313* (5793), 1642–1645.
- (10) Cheng, Y. Single-Particle Cryo-EM—How Did It Get Here and Where Will It Go. *Science* **2018**, *361* (6405), 876–880.
- (11) Murata, K.; Wolf, M. Cryo-Electron Microscopy for Structural Analysis of Dynamic Biological Macromolecules. *Biochimica et Biophysica Acta (BBA) - General Subjects* **2018**, *1862* (2), 324–334.
- (12) Renaud, J.-P.; Chari, A.; Ciferri, C.; Liu, W.; Rémy, H.-W.; Stark, H.; Wiesmann, C. Cryo-EM in Drug Discovery: Achievements, Limitations and Prospects. *Nat. Rev. Drug Discovery* **2018**, *17* (7), 471–492.
- (13) Lerner, E.; Cordes, T.; Ingargiola, A.; Alhadid, Y.; Chung, S.; Michalet, X.; Weiss, S. Toward Dynamic Structural Biology: Two Decades of Single-Molecule Förster Resonance Energy Transfer. *Science* **2018**, *359* (6373), eaan1133.
- (14) Dimura, M.; Peulen, T. O.; Hanke, C. A.; Prakash, A.; Gohlke, H.; Seidel, C. A. Quantitative FRET Studies and Integrative Modeling Unravel the Structure and Dynamics of Biomolecular Systems. *Curr. Opin. Struct. Biol.* **2016**, *40*, 163–185.

- (15) Craggs, T. D. Cool and Dynamic: Single-Molecule Fluorescence-Based Structural Biology. *Nat. Methods* **2017**, *14* (2), 123–124.
- (16) Lerner, E.; Barth, A.; Hendrix, J.; Ambrose, B.; Birkedal, V.; Blanchard, S. C.; Börner, R.; Sung Chung, H.; Cordes, T.; Craggs, T. D.; Deniz, A. A.; Diao, J.; Fei, J.; Gonzalez, R. L.; Gopich, I. V.; Ha, T.; Hanke, C. A.; Haran, G.; Hatzakis, N. S.; Hohng, S.; Hong, S.-C.; Hugel, T.; Ingargiola, A.; Joo, C.; Kapanidis, A. N.; Kim, H. D.; Laurence, T.; Lee, N. K.; Lee, T.-H.; Lemke, E. A.; Margeat, E.; Michaelis, J.; Michalet, X.; Myong, S.; Nettels, D.; Peulen, T.-O.; Ploetz, E.; Razvag, Y.; Robb, N. C.; Schuler, B.; Soleimaninejad, H.; Tang, C.; Vafabakhsh, R.; Lamb, D. C.; Seidel, C. A.; Weiss, S. FRET-Based Dynamic Structural Biology: Challenges, Perspectives and an Appeal for Open-Science Practices. *eLife* **2021**, *10*, No. e60416.
- (17) Díaz-Celis, C.; Cañari-Chumpitaz, C.; Sosa, R. P.; Castillo, J. P.; Zhang, M.; Cheng, E.; Chen, A. Q.; Vien, M.; Kim, J.; Ono, B.; Bustamante, C. Assignment of Structural Transitions during Mechanical Unwrapping of Nucleosomes and Their Disassembly Products. *Proc. Natl. Acad. Sci. U.S.A.* **2022**, *119* (33), e2206513119.
- (18) Shrestha, P.; Jonchhe, S.; Emura, T.; Hidaka, K.; Endo, M.; Sugiyama, H.; Mao, H. Confined Space Facilitates G-Quadruplex Formation. *Nat. Nanotechnol.* **2017**, *12* (6), 582–588.
- (19) Stigler, J.; Ziegler, F.; Gieseke, A.; Gebhardt, J. C. M.; Rief, M. The Complex Folding Network of Single Calmodulin Molecules. *Science* **2011**, *334* (6055), 512–516.
- (20) Petrosyan, R.; Narayan, A.; Woodside, M. T. Single-Molecule Force Spectroscopy of Protein Folding. *J. Mol. Biol.* **2021**, *433* (20), 167207.
- (21) Ying, Y.-L.; Hu, Z.-L.; Zhang, S.; Qing, Y.; Fragasso, A.; Maglia, G.; Meller, A.; Bayley, H.; Dekker, C.; Long, Y.-T. Nanopore-Based Technologies beyond DNA Sequencing. *Nat. Nanotechnol.* **2022**, *17* (11), 1136–1146.
- (22) Dietz, H.; Rief, M. Protein Structure by Mechanical Triangulation. *Proc. Natl. Acad. Sci. U.S.A.* **2006**, *103* (5), 1244–1247.
- (23) Kim, D.; Sahin, O. Imaging and Three-Dimensional Reconstruction of Chemical Groups inside a Protein Complex Using Atomic Force Microscopy. *Nat. Nanotechnol.* **2015**, *10* (3), 264–269.
- (24) Shrestha, P.; Yang, D.; Tomov, T. E.; MacDonald, J. I.; Ward, A.; Bergal, H. T.; Krieg, E.; Cabi, S.; Luo, Y.; Nathwani, B.; Johnson-Buck, A.; Shih, W. M.; Wong, W. P. Single-Molecule Mechanical Fingerprinting with DNA Nanoswitch Calipers. *Nat. Nanotechnol.* **2021**, *16* (12), 1362–1370.
- (25) Chaiet, L.; Wolf, F. J. The Properties of Streptavidin, a Biotin-Binding Protein Produced by Streptomycetes. *Arch. Biochem. Biophys.* **1964**, *106*, 1–5.
- (26) Hendrickson, W. A.; Pähler, A.; Smith, J. L.; Satow, Y.; Merritt, E. A.; Phizackerley, R. P. Crystal Structure of Core Streptavidin Determined from Multiwavelength Anomalous Diffraction of Synchrotron Radiation. *Proc. Natl. Acad. Sci. U.S.A.* **1989**, *86* (7), 2190–2194.
- (27) Le Trong, I.; Wang, Z.; Hyre, D. E.; Lybrand, T. P.; Stayton, P. S.; Stenkamp, R. E. Streptavidin and Its Biotin Complex at Atomic Resolution. *Acta Crystallogr. D Biol. Crystallogr.* **2011**, *67*, 813–821.
- (28) Yuan, C.; Chen, A.; Kolb, P.; Moy, V. T. Energy Landscape of Streptavidin–Biotin Complexes Measured by Atomic Force Microscopy. *Biochemistry* **2000**, *39* (33), 10219–10223.
- (29) Lee, G. U.; Kidwell, D. A.; Colton, R. J. Sensing Discrete Streptavidin–Biotin Interactions with Atomic Force Microscopy. *Langmuir* **1994**, *10* (2), 354–357.
- (30) Sedlak, S. M.; Schendel, L. C.; Gaub, H. E.; Bernardi, R. C. Streptavidin/Biotin: Tethering Geometry Defines Unbinding Mechanics. *Sci. Adv.* **2020**, *6* (13), eaay5999.
- (31) Gruber, S.; Löf, A.; Sedlak, S. M.; Benoit, M.; Gaub, H. E.; Lipfert, J. Designed Anchoring Geometries Determine Lifetimes of Biotin–Streptavidin Bonds under Constant Load and Enable Ultra-Stable Coupling. *Nanoscale* **2020**, *12* (41), 21131–21137.
- (32) Basu, S.; Finke, A.; Vera, L.; Wang, M.; Olieric, V. Making Routine Native SAD a Reality: Lessons from Beamline X06DA at the Swiss Light Source. *Acta Cryst. D* **2019**, *75* (3), 262–271.
- (33) Dai, J.; Punchedhewa, C.; Ambrus, A.; Chen, D.; Jones, R. A.; Yang, D. Structure of the Intramolecular Human Telomeric G-Quadruplex in Potassium Solution: A Novel Adenine Triple Formation. *Nucleic Acids Res.* **2007**, *35* (7), 2440–2450.
- (34) Hess, S. T.; Girirajan, T. P. K.; Mason, M. D. Ultra-High Resolution Imaging by Fluorescence Photoactivation Localization Microscopy. *Biophys. J.* **2006**, *91* (11), 4258–4272.
- (35) Rust, M. J.; Bates, M.; Zhuang, X. Stochastic Optical Reconstruction Microscopy (STORM) Provides Sub-Diffraction-Limit Image Resolution. *Nat. Methods* **2006**, *3* (10), 793–795.
- (36) Dokmanic, I.; Parhizkar, R.; Ranieri, J.; Vetterli, M. Euclidean Distance Matrices: Essential Theory, Algorithms, and Applications. *IEEE Signal Processing Magazine* **2015**, *32* (6), 12–30.
- (37) Weber, P. C.; Ohlendorf, D. H.; Wendoloski, J. J.; Salemme, F. R. Structural Origins of High-Affinity Biotin Binding to Streptavidin. *Science* **1989**, *243* (4887), 85–88.